Synthesis and Characterization of Layered Chlorocadmates(II) with Perovskite-like Structures

L. P. Battaglia, A. Bonamartini Corradi, and G. Pelosi

Istituto di Chimica Generale e Inorganica, Centro di Studio per la Strutturistica Diffrattometrica del C.N.R., University of Parma, 43100 Parma, Italy

M. R. Cramarossa, T. Manfredini, and G. C. Pellacani*

Dipartimento di Chimica, Facoltà di Ingegneria, University of Modena, 41100 Modena, Italy

A. Motori, A. Saccani, and F. Sandrolini

Dipartimento di Chimica Applicata e Scienza dei Materiali, Facoltà di Ingegneria, University of Bologna, 40136 Bologna, Italy

M. F. Brigatti

Istituto di Mineralogia e Petrografia, University of Modena, 41100 Modena, Italy

Received December 6, 1991. Revised Manuscript Received March 18, 1992

The synthesis and the structural, thermal, and electrical characterization of tetrachlorocadmate(II) systems, with perovskite-like structures, are described. The countercations are diprotonated amines, such as the ethylenediamine and propane-1,3-diamine dications. The structural model of the compounds consists of layers extending to the *ab* plane of $CdCl_6$ corner sharing octahedra. The holes between these layers are occupied by alkylammonium ions stabilizing the structure through hydrogen bonding. Thermal analysis shows the presence of a first-order phase transition in the propane-1,3-diammonium compound, related to the disordering of the hydrocarbon chains at high temperatures which causes a decrease in the *c* parameter and minor differences in the *a* and *b* parameters. The electrical conductivity of the investigated compounds is apparenly protonic and seems to increase as the distance between the layers containing the inorganic chains increases.

Introduction

Layered silicate clays are well recognized for their ability to form a variety of pillared intercalated derivatives[1,2] with novel properties for selective absorption and catalysis.[3-5] Two-dimensional polymeric chlorocadmates(II) have received a great deal of attention from both the theoretical and experimental points of view because of their peculiar properties, such as structural, thermal, catalytic, electrical, etc., and of the prediction of impurity electronic configurations and their lattice locations, which is a key problem in semiconductor physics.[6-8] By analogy to the layered silicates, these chlorocadmates(II) may also represent a potentially important class of lamellar ionic solids which give pillared derivatives. In this respect the Cd^{2+} ion, being a d^{10} species, is particularly suitable for designing the construction of these structural archetypes, because of its variety of coordination numbers and geometries, depending on crystal-packing, hydrogen bonding, and halide dimensions.[9,10] These materials, which present the same polarity as pillared layered silicate clays, consisting of negatively charged $CdCl_6$-like layers separated by densely intercalated chains of organic cations, can easily afford products with tailored interlayer distances depending on the cation lengths. As such, they may find practical utilization as starting materials[11] for the preparation of new pillared derivatives with gallery heights and pore sizes, such as is required for catalytic reactions of organic molecules.

In the present paper we report the synthesis and the structural, thermal, and electrical characterization of tetrachlorocadmate(II) systems having perovskite-like structures which contain diprotonated amines, such as the ethylenediamine and propane-1,3-diamine dications (enH_2 and pnH_2, respectively). The crystal and molecular structure of the $[CdCl_4](pnH_2)$ compound has been reported by Willett.[12] The present results are compared with those previously obtained for a compound having similar structure in which the inorganic layers were separated by diethylenetriamine trications ($denH_3$).[13]

Further interest arises from the fact that these materials represent unusual solid inorganic/organic composites and can serve as a model system for understanding the factors controlling the stereochemistry and polymeric nature of the metal(II) ion, as well as the correlations among symmetry, thermal, optical and electrical behavior.[13-15]

(1) Vaughan, D. E. W. *Catal. Today* **1988**, *2*, 187.
(2) Pinnavaia, T. *Science* **1983**, *220*, 365.
(3) Adams, J. M. *Appl. Clay Sci.* **1987**, *2*, 309.
(4) *Catalysis Today—Pillared Clays*; Burch, R., Ed.; Elsevier: Amsterdam, 1988, Vol. 2, No. 2-3, pp 185–368.
(5) Figueras, F. *Catal. Rev. Sci. Eng.* **1988**, *30*, 457.
(6) Mokhlisse, R.; Couzi, M.; Chanh, N. B.; Haget, Y.; Hauw, C.; Meresse, A. *J. Phys. Chem. Solids* **1985**, *46*, 187.
(7) Chanh, N. B.; Hauw, C.; Meresse, A.; Rey-Lafon M.; Ricard, L. *J. Phys. Chem. Solids* **1985**, *46*, 1413 and references therein.
(8) Bensekrane, M.; Goltzene, A.; Meyer, B.; Schwab, C.; Elwell, D.; Feigelson, R. S. *J. Phys. Chem. Solids* **1985**, *46*, 481 and references therein.
(9) Dean, P. A. W. *Progr. Inorg. Chem.* **1978**, *24*, 109 and references therein.
(10) Tuck, D. G. *Rev. Inorg. Chem.* **1979**, *1*, 209 and references therein.
(11) Landis, M. E.; Aufdembrink, B. A.; Chu, P.; Johnson, I. D.; Kirker, G. W.; Rubin, M. K. *J. Am. Chem. Soc.* **1991**, *113*, 3189 and references therein.
(12) Willett, R. D. *Acta Crystallogr.* **1977**, *B33*, 1641.
(13) Manfredini, T.; Pellacani, G. C.; Battaglia, L. P.; Bonamartini Corradi, A.; Motori, A.; Sandrolini, F. *Mater. Chem. Phys.* **1988**, *20*, 215.
(14) Manfredini, T.; Pellacani, G. C.; Battaglia, L. P.; Bonamartini Corradi, A.; Giusti, J.; Motori, A.; Saccani, A.; Sandrolini, F. *Mater. Chem. Phys.* **1989**, *24*, 215.
(15) Battaglia, L. P.; Bonamartini Corradi, A.; Peposi, G.; Cramarossa, M. R.; Manfredini, T.; Pellacani, G. C.; Motori, A.; Saccani, A.; Sandrolini, F.; Giusti, J. *Mater. Eng.* **1990**, *1*, 537.

0897-4756/92/2804-0813$03.00/0

Table I. Experimental Data for the Crystallographic Analysis of the $[CdCl_4]\bullet(enH_2)$ Compound

formula	$C_2H_{10}N_2Cl_4Cd$
MW	316.3
space group	$P2_1/a$
a/Å	7.292 (3)
b/Å	7.344 (3)
c/Å	8.609 (5)
α/deg	90
β/deg	92.74 (3)
γ/deg	90
V/Å^3	460.5 (4)
Z	2
d_{calcd}/g·cm^{-3}	2.28
d_{obs}(by flotation)/g·cm^{-3}	2.26
$F(000)$	304
temp/K	293
cryst size/mm^3	0.55 × 0.45 × 0.82
diffractometer	Siemens AED
μ/cm^{-1} (Mo Kα)	34.66
scan speed/deg min^{-1}	4.12–1.18
scan width/deg	1.5 + 0.35 tan θ
radiation/Å	Mo Kα, λ = 0.7107
θ range/deg	3–30
scan mode	ω–2θ
measd reflns	1520
condition for obsd reflns	$I > 3\sigma(I)$
no. of reflns used in the refinement	1210
min, max ht in final $\Delta\rho$/e·Å^{-3}	−0.7, 0.5
no. of ref params	63
$R = \sum\|\Delta F\|/\sum\|F_o\|$	0.034
$R_w = [\sum w(\Delta F)^2/\sum wF_o^2]^{1/2}$	0.035
k, g ($w = k/[\sigma^2(F_o) + gF_o^2]$)	15.921, 0.0195

Experimental Section

Synthesis. The crystalline compound was precipitated by mixing concentrated hydrogen chloride solutions of the ethylenediamine or propane-1,3-diamine or diethylenetriamine[13] and $CdCl_2{\cdot}2H_2O$ in 1:1 molar ratios and allowing the solutions to stand several hours. Recrystallization by slow evaporation at room temperature of concentrated hydrogen chloride solutions (12 M) gives white crystals, stable in air at room-temperature.

Elemental Analyses: $CdCl_4{\cdot}enH_2$: Found C, 7.6; H, 3.3; N, 9.0. Calcd for $C_2H_{10}N_2CdCl_4$: C, 7.6; H, 3.2; N, 8.9. $CdCl_4{\cdot}pnH_2$: Found: C, 10.8; H, 3.7; N, 8.4. Calcd for $C_3H_{12}N_2CdCl_4$: C, 10.9; H, 3.7; N, 8.5. $CdCl_5{\cdot}denH_3$: Found: C, 12.1; H, 4.1; N, 10.6. Calcd for $C_4H_{16}N_3CdCl_5$: C, 12.2; H, 4.1; N, 10.5.

Physical Measurements. Thermogravimetric and differential scanning calorimetric analyses were performed with a Mettler TG 50 thermobalance and a Perkin-Elmer DSC-2C calorimeter equipped with an IBM PS 2/30 automatic data acquisition and processing system employing sealed Al pans. The dimensional changes as a function of temperature were measured on a single crystal with a homemade instrument based on the use of a capacitive displacement transducer with a resolution better than 5×10^{-9} m. Far-infrared spectra were recorded with an FT-IR Bruker Spectrophotometer in polyethylene pellets in the 500–60-cm^{-1} spectral range. Carbon, hydrogen, and nitrogen were analyzed with a Carlo Erba Mod. 1106 elemental analyzer.

Electrical Measurements. Disks of 28-mm diameter and thickness up to 2 mm suitable for electrical measurements were compacted in vacuo under a pressure of 0.3 kN/mm^2. The samples were then gold coated by evaporation under vacuum according to the required electrode configuration and stored in a dark, vacuum environment over P_2O_5 until the electrical measurements were made. Prior to any electrical measurement the samples were sintered at 198 °C under vacuum for 8 h. A three-terminal technique was used for both direct current (dc) and alternating current (ac) measurements, in view of the rather low electrical conductivity exhibited by these compounds at room temperature. The voltmeter–ammeter method in dc and the Schering bridge method in ac measurements were used with cells and instrumentation described elsewhere, according to ASTM D 150 and D 257 standards.[16-18] Dc charging currents, under an electric field of 1000 V cm^{-1}, and discharging currents, both as a function of time, were also measured, to detect possible dielectric relaxation effects in the ultralow-frequency range after Fourier transform of the dc data.[19] All measurements were made in vacuo at constant temperature, in the frequency range 300 kHz to 10^{-2} Hz, from the highest allowed temperatures for each sample to room temperature, to avoid any possible contamination of gases or vapours on the surfaces of the samples.

Table II. Fractional Atomic Coordinates (×10^4) for Non-Hydrogen Atoms (×10^3) and for Hydrogen Atoms in the $[CdCl_4]\bullet(enH_2)$ Compound (Esd's in Parentheses)

atom	x/a	y/b	z/c
Cd	0	0	0
Cl(1)	−306 (1)	503 (1)	2939 (1)
Cl(2)	2894 (1)	2085 (1)	−399 (1)
N	−227 (6)	4832 (4)	2822 (4)
C	465 (4)	5514 (4)	4355 (3)
H1	135 (17)	504 (53)	284 (11)
H2	241 (5)	359 (64)	271 (54)
H3	466 (11)	525 (77)	222 (10)
H4	356 (5)	671 (52)	440 (56)
H5	163 (7)	555 (87)	439 (58)

Crystal Structure Determination of the $[CdCl_4](enH_2)$ Compound. Crystal data and parameters associated with data collection are summarized in Table I. The structure amplitudes were obtained after the usual Lorentz and polarization reduction and converted on absolute scale by the least-squares method. An absorption correction was not applied in view of the low absorbance (μ_r = 0.7), the absorption correction factor A^* ranging from 3.16 to 3.01 in θ values of 3–30°, assuming a nearly cylindrical shape for the crystal. The structure was solved by the heavy-atom method and refined by full-matrix least-squares cycles with anisotropic thermal parameters for non-hydrogen atoms. Hydrogen atoms were located from a ΔF map and refined isotropically. Fifteen reflections, which may have been affected by extinction or counting error, were excluded in the final refinement. Atomic coordinates for non-hydrogen atoms are listed in Table II. The final R index is 0.034; R_w is 0.035. The atomic scattering factors corrected for anomalous dispersion, were taken from International Tables.[20] Most calculations were performed on the GOULD 32/77 computer of the Centro di Studio per la Strutturistica Diffrattometrica del CNR of the University of Parma with SHELX76,[21] PARST,[22] and ORTEP,[23] programs.

XRD Powder Diffraction Measurements. XRD powder diffraction analysis was made using Philips diffractometer (Ni-filtered, Cu Kα radiation) using quartz as an internal standard. The diffractometer was equipped with a temperature control apparatus.[24] Films of uniform thickness were prepared by evaporating a suspension of 80% $CdCl_4{\cdot}pnH_2$ and 20% of quartz in absolute ethanol onto a thin aluminum sheet. The reflections were recorded with a low counter speed (0.25 deg/min) in the 2θ range 8–80° in the temperature range 24–180 °C (temperature uncertainity ±2 °C). The unit cell dimension was determined by the method of least squares starting from the model proposed by Willet[12] on 42 and 25 diffraction lines for the sample at room temperature and at 130 °C, respectively.

Results and Discussion

Crystal Structure of the $[CdCl_4](enH_2)$ Compound. The structure of the $[CdCl_4](enH_2)$ salt consists of ethylenediammonium cations and $[CdCl_4^{2-}]_n$ anions. Each

(16) Sandrolini, F. *J. Phys. E: Sci. Instrum.* **1980**, *13*, 152.
(17) Sandrolini, F.; Cremonini, P. *Mater. Plast. Elastomeri* **1979**, 405.
(18) Sandrolini, F.; Manaresi, P. *26th Int. Symp. Macromol. IUPAC, Mainz, (FRG) Sept. 17–21, 1979*; Ludenwald, I., Weis, R., Eds.; Mainz, 1979; Vol. III, p 1463.
(19) Sandrolini, F. Proc. AIM Meeting on "Electrical behavior of polymeric materials", Bologna, Italy, Mar 1–2, 1984; p 247.
(20) *International Tables For X-Ray Crystallography*; Kynoch Press: Birmingham, 1974; Vol. 4, pp 99–101 and 149–150.
(21) Sheldrick, G. SHELX 76, Program System for Crystal Structure Determination; University of Cambridge: Cambridge, 1976.
(22) Nardelli, M. *Comput. Chem.* **1983**, *7*, 95.
(23) Johnson, C. K. *Oak Ridge Natl. Lab. (Rep). ORNL (U.S.)* **1965**, ORNL-3794.
(24) Valdrè, G. *Miner. Petrogr. Acta* **1988**, *31*, 189.

Table III. Bond Distances (angstroms) and Angles (degrees) for the $[CdCl_4]\cdot(enH_2)$ Compound (Esd's in Parentheses)

Cd–Cl(1)	2.556 (1)	Cd–Cl(2)[a]	2.648 (1)
Cd–Cl(2)	2.643 (1)		
Cl(1)–Cd–Cl(2)	98.71 (3)	Cl(2)–Cd–Cl(2)[a]	91.34 (4)
Cl(1)–Cd–Cl(2)[a]	88.05 (3)	Cd–Cl(2)–Cd[a]	155.99 (4)
N–C	1.478 (5)	C–C[b]	1.528 (4)
N–C–C	109.7 (3)		

[a] $^1/_2 - x, y - ^1/_2, -z$. [b] $-x, 1 - y, 1 - z$.

Table IV. Hydrogen Bond Distances (angstroms) and Angles (deg)

N···Cl(1)	3.204 (4)	N–H(2)···Cl(1)	<165 (4)
N···Cl(1)[a]	3.273 (5)	N–H(1)···Cl(1)[a]	<160 (4)
N···Cl(2)[b]	3.213 (4)	N–H(3)···(Cl2)[b]	<167 (6)

[a] $x - ^1/_2, ^1/_2 - y, z$. [b] $^1/_2 - x, ^1/_2 + y, -z$.

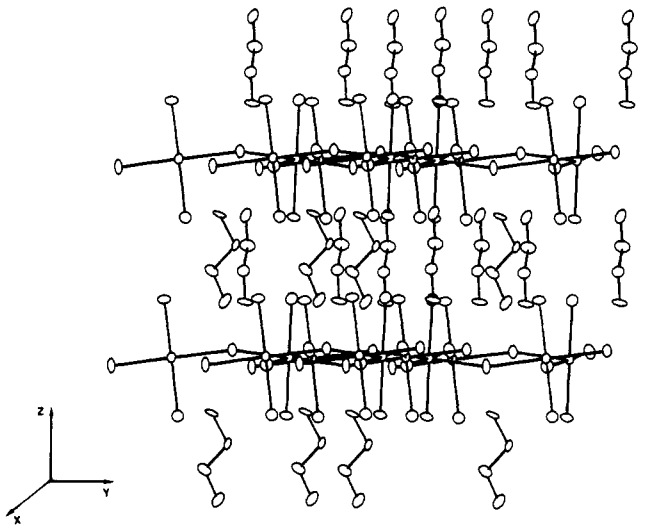

Figure 1. Network of $[CdCl_4^{2-}]$ anions in $[CdCl_4](enH_2)$ compound.

cadmium(II) atom, lying on the symmetric center, is surrounded by six chlorine atoms, two of them crystallographically independent, in a slightly distorted octahedral arrangement. The $CdCl_6$ octahedra, which shows the typical axial compression with the bridging Cd–Cl distances (2.643 (1), 2.648 (1) Å) longer than the terminal ones (2.556 (1) Å; Table III), share corners to form a two-dimensional network containing metal–halogen layers in the xy plane (Figure 1). The bond distances and angles around the cadmium atom, which are in close agreement with those observed in other similar chlorocadmate compounds, are quoted in Table III. The Cd···Cd intralayer distance is 5.145 (1) Å (Cd–Cl(2)–Cd^i = 160.00 (4); $i = ^1/_2, ^1/_2, 0$), as normally observed in chlorocadmates presenting a perovskite-like structure. The ethylenediammonium ion is planar with C–N and C–C distances typical of N sp^3 and C sp^3.

Interposed sheets of aligned ethylenediammonium cations, in the extended form, link adjacent layers through strong hydrogen bonding, involving both ends of each counterion organic moiety and the terminal coordinated chlorine ions (Figure 2). In Table IV the more relevant hydrogen bond distances and angles are reported.

The bulk structural archetype of this compound is closely similar to what was observed in $[CdCl_4](pnH_2)$[12] and $[CdCl_5](denH_3)$[13] ($denH_3$ = diethylenetriammonium trication) compounds, which differ from one another in that the interlayer Cd···Cd distances are dependent on the length of the extended ammonium cations: 8.609 (5) Å in the ethylenediammonium, 9.555 Å in the propane-1,3-diammonium, and 12.331 Å in the diethylenetriammonium chlorocadamate(II) compounds.

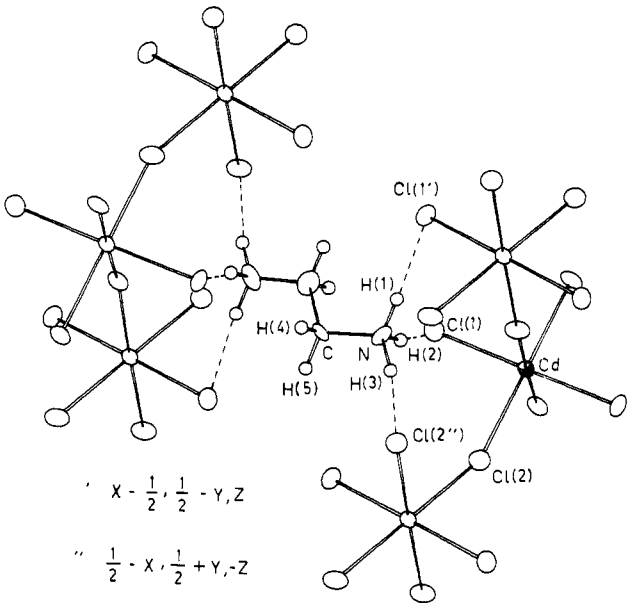

Figure 2. Perspective view of the structure of the $[CdCl_4](enH_2)$ compound.

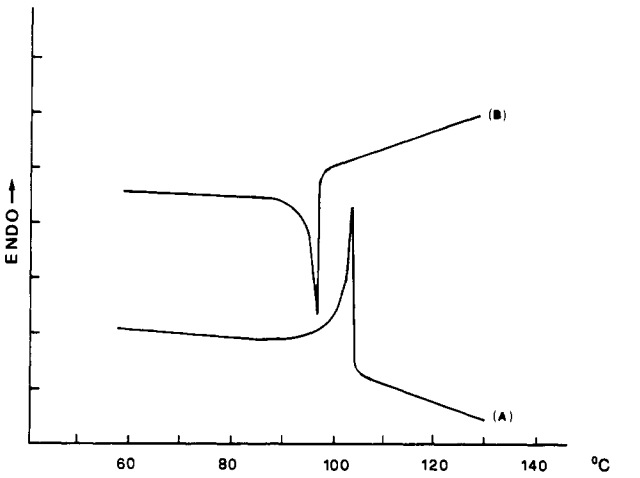

Figure 3. Thermograms of the $[CdCl_4](pnH_2)$ compound: (A) heating curve and (B) cooling curve.

Thermal Analysis Results and XRD Powder Spectra. Compounds presenting a perovskite-type structure (sequences of alternating layers of corner-sharing MX_6 octahedra), containing interposed sheets of protonated alkylmonoammonium countercations among layers, generally exhibit complex polymorphic behavior with temperature.[6,8,25]

The three compounds studied showed different thermal behavior. In fact all the compounds, investigated by thermogravimetric (TG), differential thermogravimetric (DTG), and differential scanning calorimetric (DSC) techniques, do not exhibit any weight loss up to their decomposition, which begins after the complete melting of the compounds. While DSC thermograms of the $[CdCl_4](enH_2)$ and $[CdCl_5](denH_3)$ compounds are characterized by a single endothermic melting peak at 300 and 240 °C, respectively, that of the $[CdCl_4](pnH_2)$ compound shows two endothermic peaks, which are reproduced on

(25) Kind, R.; Plesko, S.; Arend, H.; Blinc, R.; Zeks, B.; Seliger, J.; Lozar, B.; Slak, J.; Levstik, A.; Filipic, C.; Zagar, V.; Lahajnar, G.; Milia, F.; Chapuis, G. *J. Chem. Phys.* **1979**, *71*, 2118.

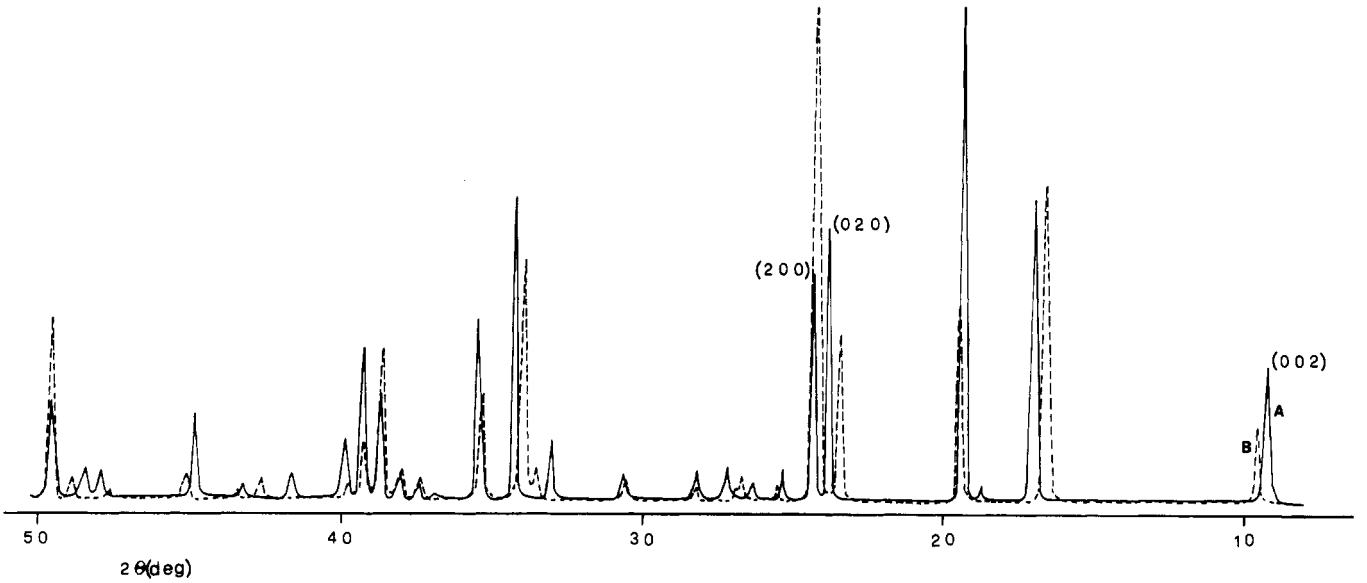

Figure 4. XRD patterns of the $[CdCl_4](pnH_2)$ compound below (a) and above (B) the phase transition temperature.

cooling (Figure 3). The first peak, which occurs at 101 °C on heating and at 97 °C on cooling with a ΔH = 0,44 kcal mol^{-1}, may be a first-order phase transition. On the basis of proton nuclear magnetic resonance (NMR) absorption and proton spin–lattice relaxation time measurements as a function of temperature, this transition, which exhibits no thermal hysteresis, was previously assigned as second order.[26] The second transition, beginning at 320 °C, corresponds to the melting point of the $[CdCl_4](pnH_2)$ compound, as confirmed by optical microscopy observations. Repeated heating–cooling cycles between 30 and 150 °C demonstrated the reproducibility of these transitions.

To unambiguously identify the crystalline phases of the $[CdCl_4](pnH_2)$ compound, their XRD patterns were recorded in the temperature range 25–130 °C. Figure 4 shows the XRD patterns at 25 and 130 °C. An indexed powder pattern for the low-temperature phase (space group *Pnma*) is given in Table V. The calculated unit cell parameters a = 7.352 (2), b = 7.503 (2), c = 19.051 (5) Å, and V = 1051.0 (4) Å^3 are in good agreement with those reported by Willet from a single-crystal analysis.[12]

On increasing the temperature, changes in the XRD patterns begin at 95 °C and are characterized by the following: (1) Shift of (00l) reflections toward lower d values (see, for example, (002)). (2) Shift of (0k0) reflections toward higher d values (see, for example, (020)). No shift was observed for (h00) reflections (see for example (200)), whereas their intensity increases. (3) Modifications in the interplanar distances are observed for reflections involving k and l indices. All these considerations emphasize that the high-temperature phase still maintains the orthorhombic symmetry.

On the basis of these assumptions, indexing 25 reflections of the high-temperature phase powder pattern, using the parameters of the low-temperature phase, yields the following unit cell parameters: a = 7.351 (5), b = 7.622 (7), c = 18.57 (1), (1), V = 1040 (1) for the high-temperature phase. The indexed powder pattern for the high-temperature phase is reported in Table VI.

The structural model for the $[CdCl_4](pnH_2)$ compound[12] consists of layers extending in the ab plane of the $CdCl_6$ corner-sharing octahedra. The holes between these layers are occupied by alkylammonium ions stabilizing the structure through hydrogen bonding. The pnH_2 ions in

Table V. Indexed Powder Pattern for Low-Temperature Phase $[CdCl_4](pnH_2)$ Compound

$h\ k\ l$	d_{obs}	d_{calc}	I/I_{max}
0 0 2	9.490	9.526	27
1 1 0	5.240	5.252	61
0 0 4	4.760	4.763	3
1 1 2	4.592	4.599	100
0 2 0	3.748	3.752	55
2 0 0	3.676	3.676	44
1 1 4	3.527	3.528	6
0 1 5	3.400	3.397	3
1 2 1	3.290	3.292	7
2 0 3	3.180	3.182	6
2 1 3	2.930	2.929	5
2 0 4	2.913	2.910	5
1 1 6	2.720	2.717	12
2 2 0	2.626	2.626	60
0 1 7	2.563	2.558	1
2 2 2	2.533	2.531	37
1 2 5	2.513	2.512	1
2 0 6	2.406	2.403	3
0 0 8	2.386	2.381	6
1 3 0	2.369	2.368	8
3 1 0	2.331	2.330	21
2 2 4	2.300	2.300	29
3 1 2	2.266	2.263	12
1 1 8	2.168	2.169	5
1 3 4	2.120	2.120	7
3 1 4	2.091	2.093	3
2 2 6	2.022	2.024	17
2 0 8	2.000	1.999	1
2 3 4	1.897	1.897	5
3 1 6	1.878	1.878	5
4 0 0	1.838	1.838	20
4 0 1	1.823	1.830	2
1 4 0	1.820	1.818	3
4 0 2	1.804	1.805	6
2 1 9	1.783	1.782	2
2 2 8	1.764	1.764	9
1 4 3	1.750	1.746	3
0 4 4	1.745	1.745	6
3 3 2	1.721	1.722	4
1 3 8	1.679	1.679	2
3 1 8	1.666	1.665	3
2 1 10	1.651	1.650	4

a	7.352 (2) Å
b	7.503 (2) Å
c	19.051 (5) Å
vol	1051 (4) Å^3

(26) Blinc, R.; Burgar, M.; Lozar, Seliger, J; Slak, J.; Rutar, V. B.; Arend, H.; Kind, R. *J. Chem. Phys.* **1977**, *66*, 278.

Table VI. Indexed Powder Pattern for High-Temperature Phase $[CdCl_4](pnH_2)$ Compound

h k l	d_{obs}	d_{calc}	I/I_{max}
0 0 2	9.250	9.286	15
1 1 0	5.290	5.292	64
0 0 4	4.620	4.643	2
1 1 2	4.600	4.600	39
0 2 0	3.810	3.811	33
2 0 0	3.675	3.676	100
1 1 4	3.500	3.490	3
0 1 5	3.345	3.339	5
1 2 1	3.328	3.328	2
2 0 3	3.160	3.161	2
2 1 3	2.921	2.920	4
1 1 6	2.675	2.672	7
2 2 0	2.645	2.646	50
2 2 2	2.543	2.545	22
1 3 0	2.400	2.401	4
2 0 6	2.371	2.368	5
3 1 0	2.330	2.333	29
2 2 4	2.300	2.299	10
3 1 2	2.265	2.263	2
1 1 8	2.130	2.126	4
3 1 4	2.085	2.085	1
2 2 6	2.013	2.011	5
2 3 4	1.906	1.905	1
3 1 6	1.864	1.863	4
4 0 0	1.837	1.838	37

a	7.351 (5) Å
b	7.622 (7) Å
c	18.57 (1) Å
vol	1040 (1) Å^3

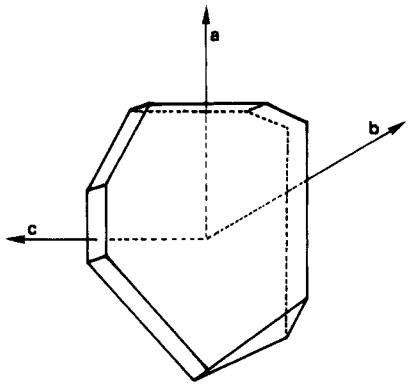

Figure 5. Orientation of one $[CdCl_4](pnH_2)$ crystal.

this compound are well ordered, while in the analogous Mn(II) and Fe(II) complexes[27] no evidence of ordering occurs. The disorder in the Mn(II) and Fe(II) compounds is reflected in a decrease in the c parameter and in a major difference in the a and b parameters. Taking into account the different metal radii, similar structural characteristics are found for the Cd(II) higher temperature phase. Therefore the structural phase transition observed in the $[CdCl_4](pnH_2)$ compound may be associated with the disordering of the hydrocarbon chains at higher temperatures, in agreement with the results previously obtained on this and similar compounds through proton NMR studies.[26]

Dimensional variation measurements performed on $[CdCl_4](pnH_2)$ crystals at different temperatures confirm the XRD results. A lengthening along one direction (b in Figure 5) was observed near the transition temperature in big lamellar crystals: along the same direction, the crystals appear brittle and easy to cleave, and a shortening takes place along the spatial direction indicated as c in Figure 5. The a, b, and c directions in Figure 5 correspond to the a, b, and c structural axes, as experimentally determined.

(27) Willett, R. D.; Riedel, E. F. *Chem. Phys.* **1975**, *8*, 112.

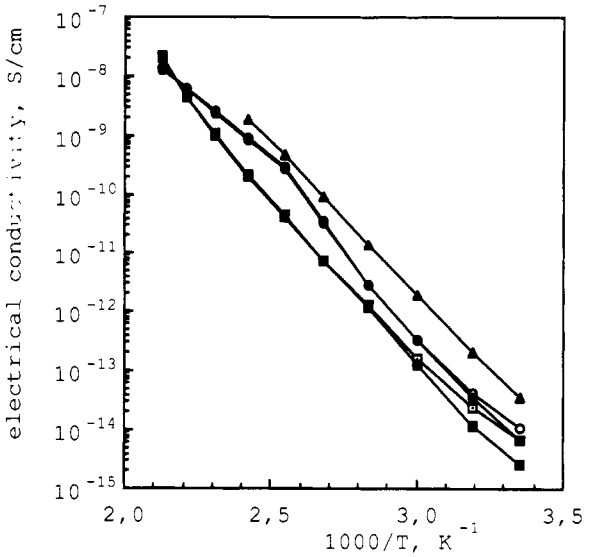

Figure 6. Electrical conductivity σ of $[CdCl_4](enH_2)$ (□), $[CdCl_4](pnH_2)$ (○), and $[CdCl_5](denH_3)$ (△) compounds as a function of reciprocal absolute temperature at 1 (open symbols) and 60 (fitted symbols) min after the voltage application.

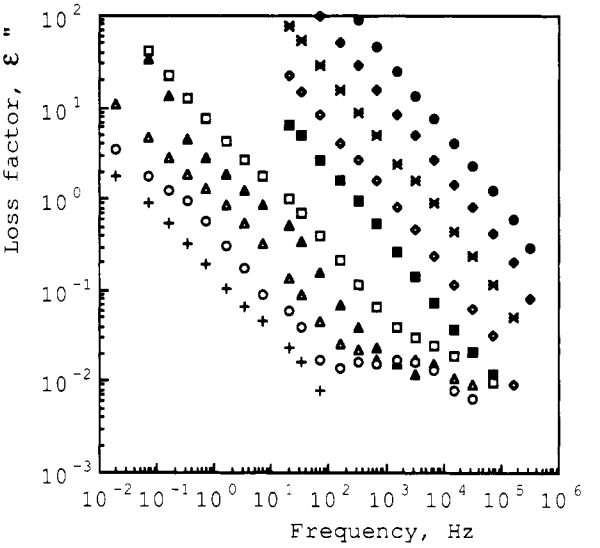

Figure 7. Loss factor of $[CdCl_4](enH_2)$ vs frequency vs temperature [T = 198 (●), 180, (◆), 160 (✱), 140 (◇), 120 (■), 100 (□), 80 (▲), 60 (△), 40 (○), 25 °C (+)].

Electrical Results. The electrical conductivity σ calculated at 1 and 60 min after the application of a step voltage for the two compounds is plotted vs the reciprocal absolute temperature in the temperature range 25–198 °C as shown in Figure 6, where data at 1 min for $denH_3$ are reported for the sake of comparison.

The compounds can be classified as insulators at room temperature: however, their conductivity strongly increases with temperature, reaching the semiconducting range in some cases. The dc temperature dependence is nearly linear in log σ vs $1/T$ for enH_2 compound, with an activation energy of 0.49 eV, while the pnH_2 compound shows a more complex behavior, changing its slope near 100 °C, which may be related to the above-mentioned transition. Transient phenomena are almost absent except at the lowest temperatures. The electrical conductivity of the pnH_2 compound is higher than that of the enH_2 derivative at all temperatures. Measurements performed at room temperature on both samples of enH_2 and pnH_2 compounds, after the adsorption of a slight amount of

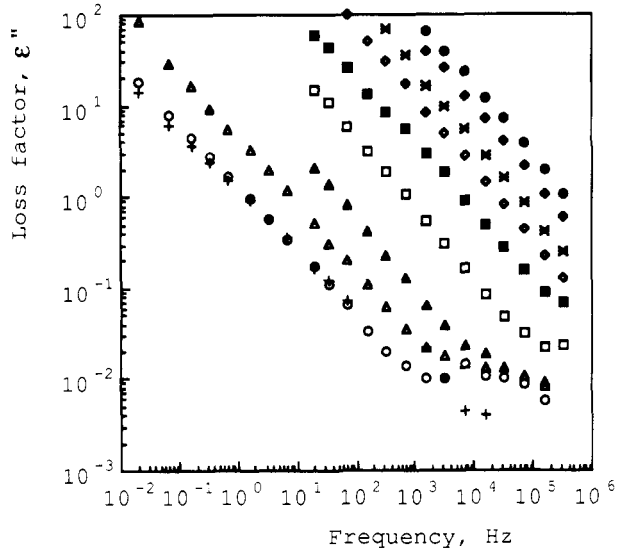

Figure 8. Loss factor of $[CdCl_4](pnH_2)$ vs frequency vs temperature [T = 198 (●), 180 (◆), 160 (✱), 140 (◇), 120 (■), 100 (□), 80 (▲), 60 (△), 40 (○), 25 °C (+)].

moisture, showed a strong increase of conductivity (3 orders of magnitude for an absorption of about 0.6 wt % of water). Dielectric measurements in the frequency range 10^{-2}–10^5 Hz at constant temperature showed no remarkable relaxation effects (Figures 7 and 8).

The relative dielectric constant (not shown for brevity) increases with temperature and decreases with frequency at all the investigated temperatures, reaching at the higher frequencies a value of about 7 for enH_2 at all temperatures and from 7 to 10 for pnH_2 as temperature increases. Also the loss factor for the two compounds at constant temperature increases with decreasing frequency, that of pnH_2 always being slightly higher than that of enH_2 at all temperatures. The Fourier transform of the discharging currents showed no relaxation processes of the Maxwell–Wagner–Sillars type.

The whole electrical behavior of the enH_2 and pnH_2 compounds is similar to that of the $denH_3$ one previously studied.[13] The electrical conductivity is lower, but the general plot and the energy of activation are almost the same. Loss factor values are lower but again the general trend is the same. An ionic mechanism of conduction based on the migration of protons onto the N atom at the center of the countercation was proposed for $denH_3$, supported by the large increase of dc electrical conductivity exhibited after moisture absorption.

In the enH_2 and pnH_2 compounds no protonated N atoms involved in weak hydrogen bonds are present in the center of the countercation as they are in the $denH_3$ one: hence their conductivity should be lower than in the $denH_3$ compound, as confirmed by the experimental data (Figure 6). Nevertheless, the conductivity in the two compounds must still be ascribed to protons present at the terminal nitrogen atom of the countercations, since conductivity greatly increases after even slight water absorption. The fact that the conductivity of the enH_2 and pnH_2 compounds is lower than in $denH_3$ confirms the interpretation previously[13] advanced that protons involved in strong hydrogen bonds (such as those at the end of the countercation) are less effective for conduction than those weakly bonded (like those present at the countercation center). An electronic mechanism cannot be ruled out as contributing to the electrical conductivity at low temperatures.

It is noteworthy that the conductivity increases with the distance between the layers containing the anionic chains (8.6 Å for enH_2, 9.5 Å for pnH_2 below 100 °C and 9.28 Å over 100 °C, 12.3 Å for $denH_3$). The slope change detectable in the plot of pnH_2 conductivity, at a temperature close to that of the order–disorder transition, may be related to the closer packing of the structure that takes place at high temperature, reducing the distance between anionic planes: as is well-knonw, such phenomena tend to oppose the ionic mechanism of conduction.

Conclusions

All of the three compounds ($[pnH_2](CdCl_4)$, $[enH_2](CdCl_4)$, and $[denH_3](CdCl_5)$) are characterized by a network of polymeric chlorocadmate(II) layers, linked one another by interposed sheets of aligned ammonium cations in the extended form. The hydrogen-bonding ability of both ends of the ammonium cations strongly anchors adjacent layers and leads to very compact and rigid structures, which are thermally stable up to the melting temperature of the compounds. The structural phase transition observed for the $[CdCl_4](pnH_2)$ compound may be associated with the disordering of the hydrocarbon chains at higher temperatures, in agreement with what is found for similar compounds having as countercations diprotonated amine cations presenting a number of carbon atoms in the chain ≥ 3.[25] The $CdCl_4$ layers play the role of stable but elastic matrices and affect the phase transition only indirectly by both linear or nonlinear coupling.

The electrical conductivity in the investigated compounds is due to the protons probably through a mechanism of migration; their conductivity is somewhat lower than that observed in the $denH_3$ compound, the protons being engaged only in strong hydrogen bonds in the structure of the investigated compounds.

The electrical conductivity increase also seems to be related to the distance increase between the layers containing the anionic chains.

Acknowledgment. Financial support (60%) from the MURST is gratefully acknowledged.

Registry No. $[CdCl_4](enH_2)$, 61949-61-9; $[CdCl_4](pnH_2)$, 61949-62-0; $[CdCl_5](denH_3)$, 56585-95-6.

Supplementary Material Available: Table of anisotropic and isotropic thermal parameters and atomic coordinates for hydrogen atoms (1 page); list of observed and calculated structure factors for [enH2]($CdCl_4$) compound (7 pages). Ordering information is given on any current masthead page.